continued

So $r = 1.77$ m. Depth to top of sphere $d = 2.87 - 1.77 = 1.10$ m. *An air-filled cavity of this size so close to the surface could constitute a hazard*

Box 2.20 Smith Rules

(1) Where the entire anomaly has been isolated:

$$d \leqslant C.\ \Delta g_{max}/\Delta g'_{max}$$

where $C = 0.65$ for a 2-D body and $C = 0.86$ for a 3-D body.

(2) When only part of an anomaly is isolated, for any point x:

$$d \leqslant K\ \Delta g_x/\Delta g'_x$$

where $K = 1.00$ for a 2-D body and $K = 1.50$ for a 3-D body.

(3) For a maximum density contrast $\delta\rho_{max}$ and a maximum value of the second horizontal gradient ($\Delta g''_{max}$) (that is, the rate of change of $\Delta g'$ with x):

$$d \leqslant 5.4\, G\delta\rho_{max}/\Delta g''_{max}.$$

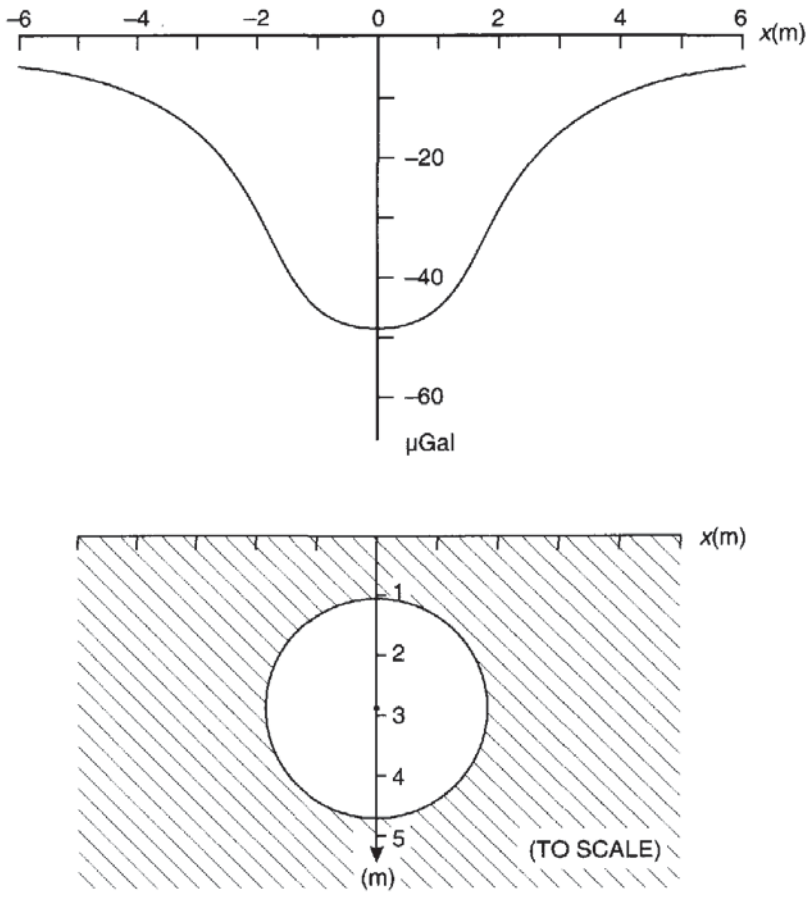

Figure 2.29 Gravity anomaly over an air-filled cavity of radius 1.77 m and 2.87 m depth to centre, in rock of density 2.5 Mg/m^3

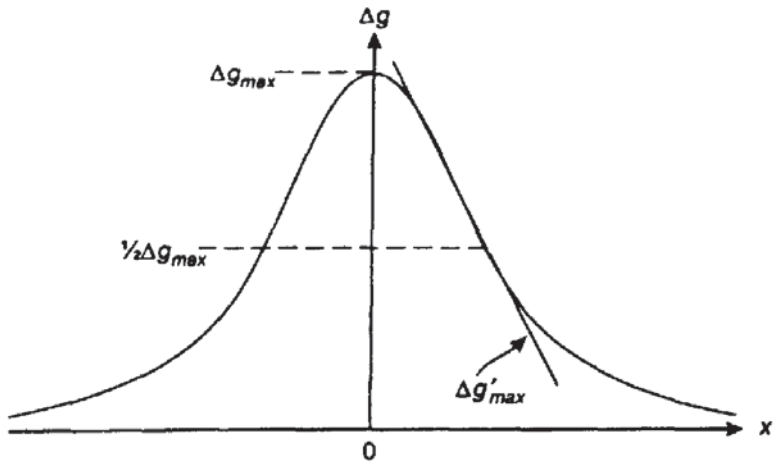

Figure 2.30 Limiting depth calculations: half-width method and gradient–amplitude ratio method (see text for details)

The third Smith Rule adopts a second-derivative method which uses the rate at which the gravity gradient changes along the profile. It is thought that second-derivative methods produce more accurate estimates of limiting depths. Second derivatives are discussed in more detail in Section 2.6.5.

2.6.4 Mass determination

Anomalous mass is the difference in mass between a geological feature and the host rock. There are two basic methods of calculating either an excess mass due to a high-density body or a mass deficiency caused by a body with a lower density.

The first method uses a rule of thumb based on the gravity anomaly half-width ($x_{1/2}$) and an assumption that the geological feature approximates to a given geometric form, such as a sphere (Box 2.21). The anomalous mass can be calculated by subtracting the mass due to a sphere (density times volume) from the mass estimated using gravity data. In the example below, the actual mass of an air-filled cavity is negligible, so the mass deficiency calculated is the mass of the missing rock.

Box 2.21 Mass of a sphere

Total mass $M \approx 255\ \Delta g_{max} (x_{1/2})^2$ tonnes

where Δg_{max} is in mGal and $x_{1/2}$ in metres.

Example

For an air-filled cavity described in Box 2.19B, the total mass deficiency of the sphere is equal to the mass of the rock that

continued

continued

would have been in the cavity, times its density (2.5 Mg/m^3):

$$\text{Mass} = \text{density} \times \text{volume} = 2.5 \times (4/3)\pi\ 1.77^3 = 58 \text{ tonnes.}$$

Using the gravity data:

$$\text{Mass} \approx 255 \times 0.048 \times 2.2^2 = 59 \text{ tonnes.}$$

The second method is based on Gauss's Theorem in potential theory (Grant and West 1965) and is particularly important for two reasons. First, the total anomalous mass of a geological feature can be calculated from the associated gravity anomaly without any assumptions being necessary about the body's shape or size. Secondly, the total anomalous mass can be very important in the determination of tonnage of ore minerals (Hammer, 1945). For this method to work effectively, it is important that the regional gravity field be removed and that the entire residual anomaly be isolated clearly. The survey area is divided into a series of rings each of which is further divided into segments of area δA. The gravity effect of each segment is determined and the total for each ring is obtained and summed together (Box 2.22). Having determined the excess mass, it is then a simple matter to calculate the actual mass (M) if the densities of the host rock (ρ_0) and the anomalous body (ρ_1) are known.

Box 2.22

(1) Total anomalous mass (M_E):

$$M_E = 23.9\Sigma(\Delta g \delta A) \text{ tonnes}$$

where Δg is in mGal and δA in metres.

(2) Actual mass of a geological body (M):

$$M = M_E \frac{\rho_1}{(\rho_1 - \rho_0)} \text{ tonnes } (\rho_1 > \rho_0).$$

Parasnis (1966) gives an example where the total anomalous mass of the Udden sulphide orebody in northern Sweden was calculated to be 568 820 tonnes. Assuming the densities of the ore and host rock to be 3.38 and 2.70 Mg/m^3 respectively, the actual mass of the ore was found to be 2.83 million tonnes, a value consistent with drillhole estimates.

2.6.5 Second derivatives

2.6.5.1 Second vertical derivative (SVD) maps

One of the problems inherent within the interpretation of Bouguer anomaly maps is that it is difficult to resolve the effects of shallow structures from those due to deeper seated ones. The removal of the effect of the regional field from the Bouguer anomaly data results in an indeterminate and non-unique set of residuals. It is possible to separate the probable effects of shallow and deeper structures by using second vertical derivatives.

The gravity field (g) which is measured by gravimeters varies with height; that is, there is a vertical gradient ($\delta g/\delta z = g'$). Over a non-uniform earth in which density varies laterally, the vertical gradient changes and the *rate* of change ($\delta g'/\delta z$) is thus the second vertical derivative of the gravity field ($\delta^2 g/\delta z^2$. This quantity is very sensitive to the effects of shallow features (and to the effects of noise and topography).

As an illustration of how the gravity effects of shallow and deep structures can be separated, consider two equal point masses (m) at two different depths, say at depths of 1 unit and 4 units. The value of g for a point mass at a depth z is simply equal to the product of the gravitational constant (G) and the mass divided by the depth z squared, so $g = Gm/z^2$). If this is differentiated twice with respect to z, it becomes $g'' = 6Gm/z^4$. This tells us that the second derivative of the two masses, g'', is inversely proportional to z^4. Hence the ratio of the two derivatives will be, for $z_1 = 1$ and $z_4 = 4$, $g''_1/g''_4 = 256$.

It is possible to compute and plot maps of the second vertical derivative of Bouguer anomaly data. The zero-contour should indicate the edges of local geological features. The contours have units where 10^{-6} mGal/cm$^2 \equiv 10^{-9}$ cm^{-1} s$^{-2} \equiv 1$ E cm^{-1}. (E stands for an Eötvös unit $= 10^{-6}$ mGal/cm, which is a measure of gravitational gradient.)

It should be emphasised that it is not possible to undertake any quantitative analyses of SVD maps except to produce characteristic profiles over known geometric forms. The main advantage of SVD maps is to highlight and clarify features spatially, as can be seen from Figures 2.31 and 2.32. In the first of these, the Bouguer anomaly map appears to have a consistent trend in the direction of the gravity gradient (increasingly positive to the east) with isogals aligned in a NW–SE direction. There is no obvious major feature evident on the Bouguer anomaly map. In contrast, the SVD map shows a major ENE–WSW linear feature with three closures, and it has picked out the outline of the Cement field in Oklahoma extremely well. Figure 2.32 illustrates the case when a single Bouguer anomaly is really the envelope of several smaller anomalies. In this atypical and rather extreme case, several deep boreholes were drilled on the large minimum indicated on both the Bouguer and the residual anomaly maps;

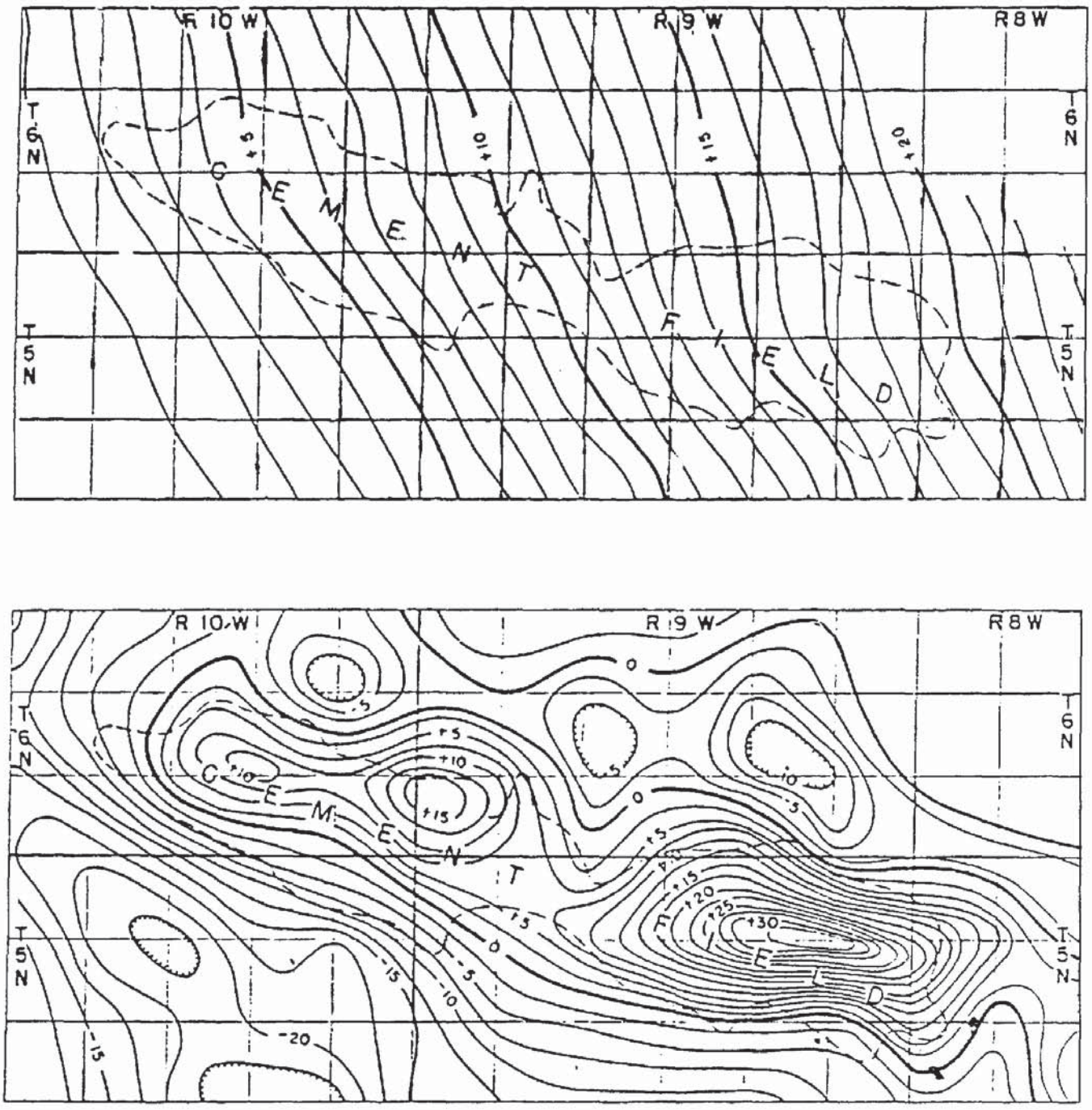

Figure 2.31 Observed Bouguer anomaly (contour interval 1 mGal) and second vertical derivative (contour interval 2.5×10^{-15} c.g.s.u.) maps over a Cement field in Oklahoma. From Elkins (1951), by permission

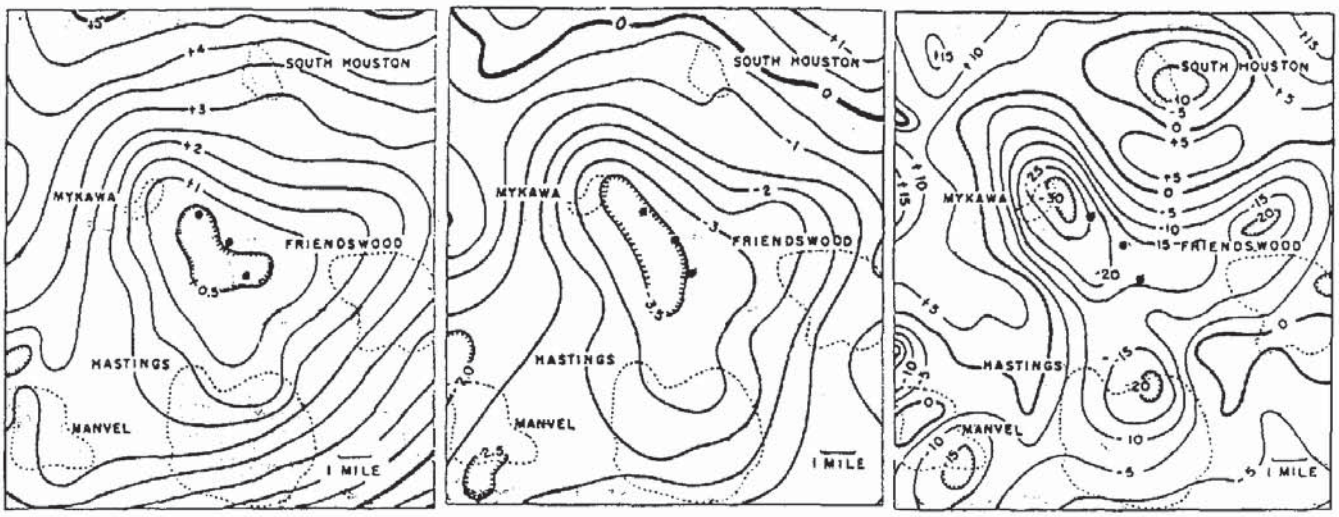

Figure 2.32 (A) Observed gravity, (B) residual gravity (contour interval 0.5 mGal), and (C) second vertical derivative (contour interval 5×10^{-15} c.g.s.u.) maps for Mykawa, Texas Gulf Coast. • indicate dry boreholes. From Elkins (1951), by permission

they were found to be dry, having missed the appropriate target, presumed to be a single salt dome. In contrast, the SVD map highlights three salt domes accurately.

Unfortunately, SVD also amplifies noise and so can produce many second-derivative anomalies that are not related to geology. Consequently, in some cases, SVD analyses provide no real advantage over the Bouguer anomaly map. An example of where extraneous anomalies shroud the geologically related features is given in Figure 2.33. Although it is possible to see on the SVD map the two main features present on the Bouguer anomaly map of the J-jaure titaniferous iron-ore region in Sweden, the SVD map also has a number of small maxima and minima that are of no structural interest. To resolve which anomalies are of geological importance, it is necessary to go back to the original gravity map and to any other source of geological information. It may even be prudent to refer back to the raw observations and corrections.

2.6.5.2 *Downward and upward continuation*

The effect on gravity of a geological mass at considerable depth is far less than if it were close to the surface (see Figure 2.24). the *principle of continuation* is the mathematical projection of potential field data (gravity or magnetic) from one datum vertically upwards or downwards to another datum. Effectively, the continuation process simulates the residual Bouguer anomaly at levels below or above sea level as if the gravity data had been obtained at those levels.

Upward continuation is relatively straightforward as the projection is usually into free space. Upward continuation serves to filter out the shorter-wavelength anomalies and reduce their amplitudes and decrease noise.

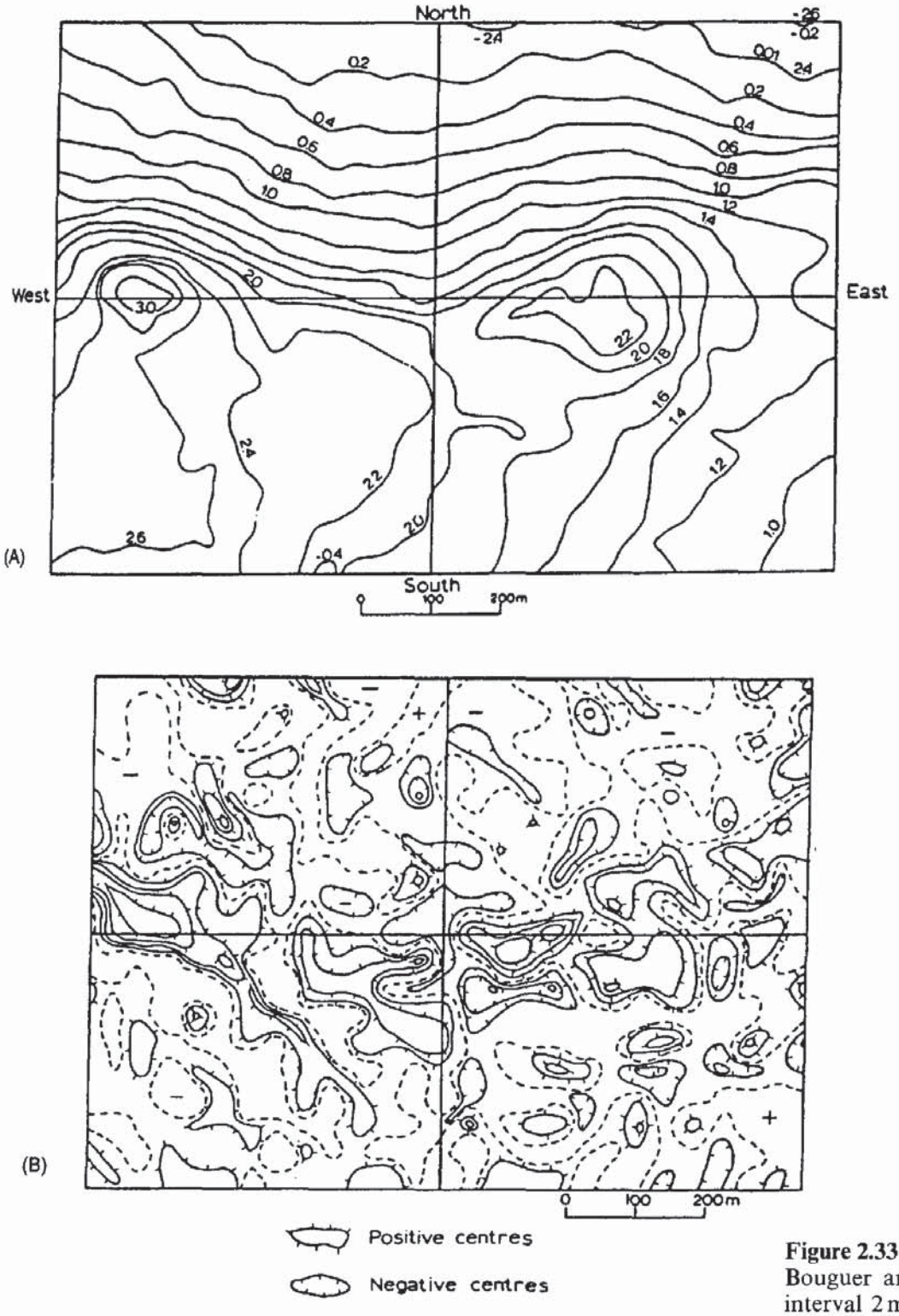

Figure 2.33 An example where the Bouguer anomaly map (A) (contour interval 2 mGal) exhibits more detail than the corresponding second vertical derivative map (B) for the J-jaure titaniferous iron-ore region in Sweden. Contours: 0 (dashed), ± 0.1, ± 0.2, ± 0.4 in units of 0.0025 mGal/m^2). From Parasnis (1966), by permission

Downward continuation is far more problematical as there is an inherent uncertainty in the position and size of the geological features as represented by the Bouguer gravity data. Furthermore, downward continuation aims to reduce each anomaly's wavelength and increase its amplitude. This mathematical amplification will also work on noise within the data and the resultant information may prove unsuitable for further analysis.

Continuation also forms a method of gravitational stripping (Hammer, 1963) where the gravity effects of upper layers are necessarily removed to reveal the anomalies due to deeper seated geological structures (e.g. Hermes 1986; Abdoh *et al.* 1990). The method uses the concept of an equivalent stratum (Grant and West, 1965). The Bouguer gravity field is continued downwards to a level that corresponds to a previously identified interface, such as from seismic reflection surveys, and an equivalent topographic surface is constructed at that level. This equivalent stratum should account for any residual anomalies at the surface arising from the interface. Continuation is discussed in much more detail by Grant and West (1965) and by Telford *et al.* (1990).

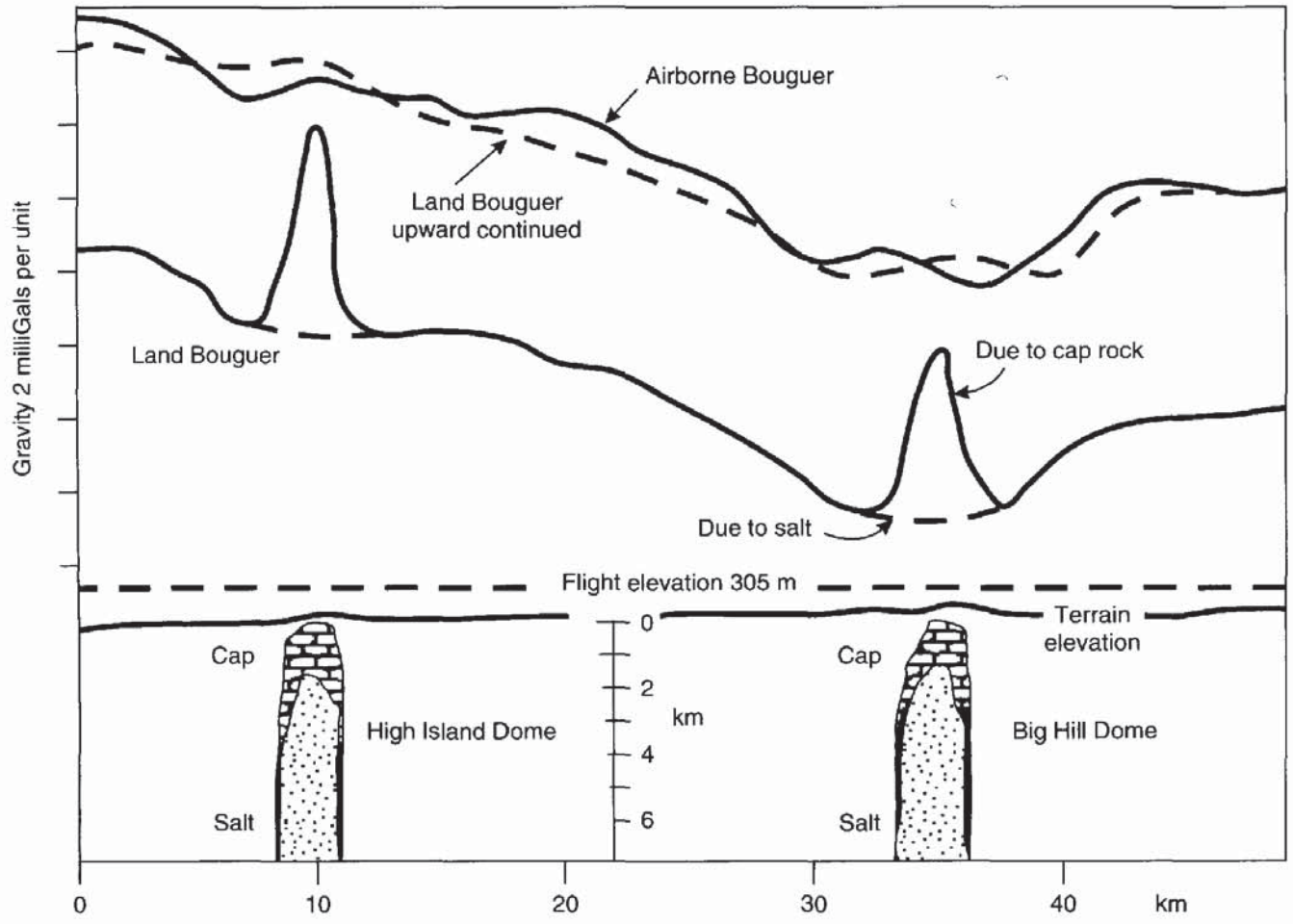

Figure 2.34 Comparison of airborne and upward continued land Bouguer gravity data with those obtained by airborne gravity surveying. From Hammer (1984), by permission

Upward continuation is used in comparisons of ground-based gravity anomalies with airborne data. It is usual to continue ground data upwards rather than to work downwards so as not to amplify noise. An example of such a comparison is shown in Figure 2.34 (Hammer 1982, 1984). Two gravity minima associated with low-density salt have shorter-wavelength maxima superimposed which are due to the high-density cap rocks. These maxima attenuate with increased elevation and the agreement between the upwardly continued land Bouguer data and the airborne is better than 5 g.u. except in the immediate vicinity of the cap rocks.

One of the major considerations in the interpretation of particularly regional gravity data is the amount of computer processing required. Considerable effort has been expended in developing computer-based methods of data enhancement. For example, image processing of data on computer-compatible tapes (CCTs) permits considerable manipulation of the data for display purposes to aid analysis and interpretation. Processes include edge enhancement to highlight lineaments (e.g. Thurston and Brown 1994), amplitude displays and spectral modelling (Figure 2.35). It is usually only economically viable to undertake such sophisticated processing on very large data sets.

Figure 2.35 Structural analysis, based on lineations from a series of colour and greyscale shaped-relief images of geophysical data can provide a basis for reassessment of regional structure, mineralisation potential and fracture patterns. This image is of observed regional Bouguer gravity data, over an area of 200 km × 140 km of the Southern Uplands. Scotland (C: Carlisle; E: Edinburgh). The data have been reduced to Ordnance Datum using a density of 2.7 Mg/m^3, interpolated to a square grid of mesh size 0.5 km and displayed as a greyscale shaded-relief image. Sun illumination azimuth and inclination are NE and 45° respectively. A series of NE trending features paralled to the regional strike and the Southern Uplands fault have been suppressed by the NE illumination, whereas subtle NW trending features linked to development of the Permian basins are enhanced and seen to be more extensive. For comparison, see Figure 3.48. Image courtesy of Regional Geophysics Group, British Geological Survey

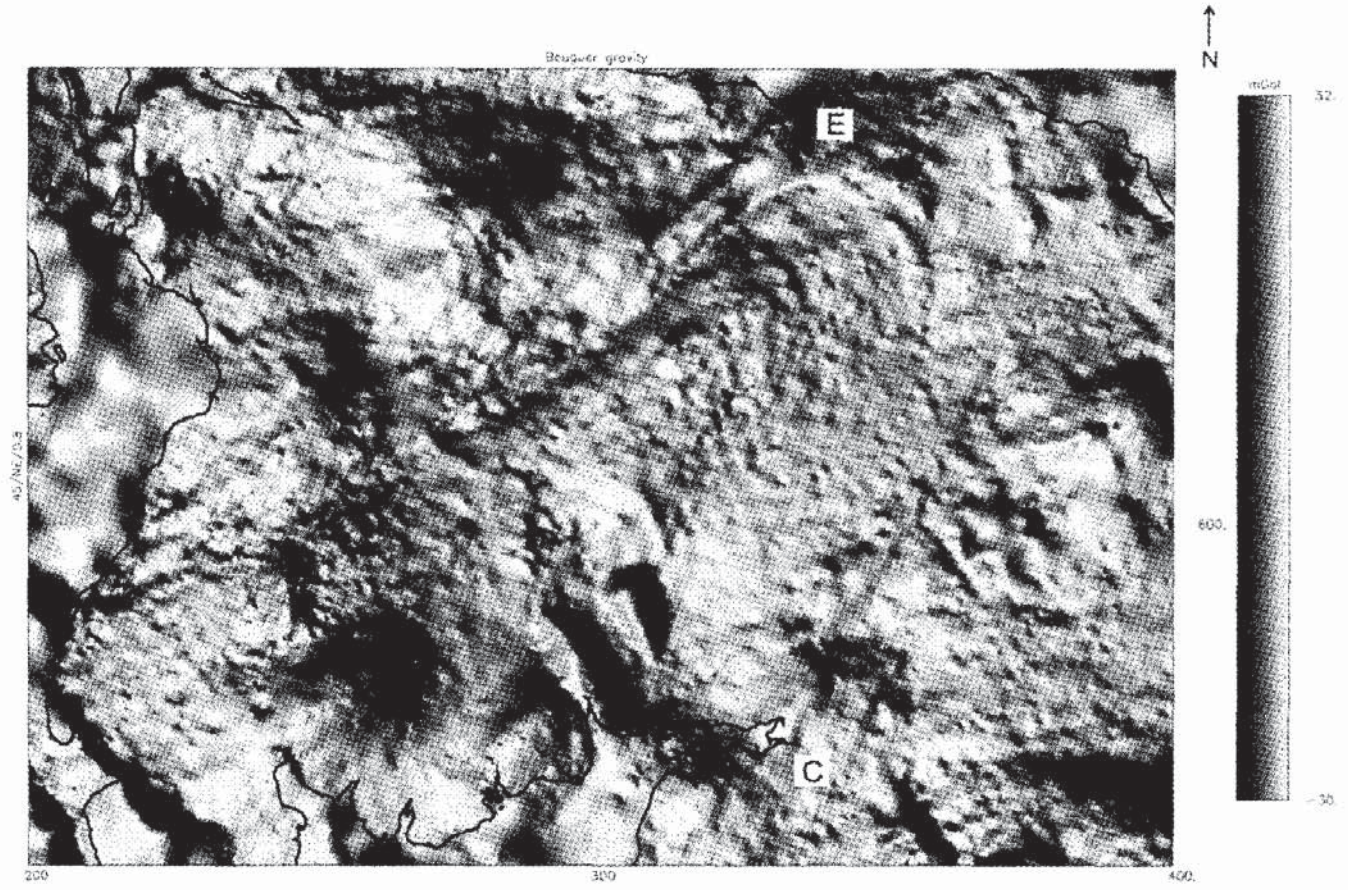

2.6.6 Sedimentary basin or granite pluton?

It is very important in the interpretation of gravity data for hydrocarbon exploration to be able to distinguish between a sedimentary basin (a good possible hydrocarbon prospect) and a granitic pluton (no prospect for hydrocarbons), as both can produce negative gravity anomalies of comparable magnitude.

For example, Arkell (1933) interpreted a minimum in an initial Bouguer gravity survey in the Moray Firth, north-east Scotland, as being due to a granite pluton. It was only after further geological work (Collette, 1958) and gravity work (Sunderland, 1972) that it was realised that the minimum was due to a sedimentary basin. Simultaneously, the Institute of Geological Sciences undertook seismic reflection surveys and initiated some shallow drilling. It was not until 1978 that the Beatrice Field was discovered (McQuillin *et al.* 1984). Had the 1933 interpretation been different, the history of the development of the North Sea as a major hydrocarbon province might have been very different.

In 1962, Bott proposed a set of criteria to distinguish between a sedimentary basin and a granite boss as interpretations of gravity minima. His argument was based on the second vertical derivative of the gravity anomaly due to a semi-infinite two-dimensional horizontal slab with a sloping edge. He found that the ratio of the moduli of the maximum and minimum second vertical derivative ($|g''_{max}|/|g''_{min}|$) provides a means of distinguishing between the two geological structures, as outlined in Box 2.23 and illustrated in Figure 2.36. McCann and Till (1974) have described how the method can be computerised, and the application of Fourier analysis to Bott's method. Some authors calculate the second *horizontal* derivative ($\delta^2 g/\delta x^2$) (e.g. Kearey and Brooks 1991; figure 6.19) which responds in exactly the same way as the *vertical* derivative except that the maxima and minima are reversed, as are the criteria in Box 2.23. In order for the method to work, the gravity anomaly attributed to the appropriate geological feature (sedimentary basin or granitic pluton) needs to be clearly isolated from adjacent anomalies due to other features. The method is not applicable, however, in cases where extensive tectonic activity has deformed either a sedimentary basin by basin-shortening or a granitic pluton by complex faulting, thereby changing the gradients of the flanks of both types of model.

Box 2.23 Bott criteria (see also Figure 2.36)

(1) For a sedimentary basin:

$$|g''_{max}|/|g''_{min}| > 1.0.$$

Basin sides slope *inwards.*

continued

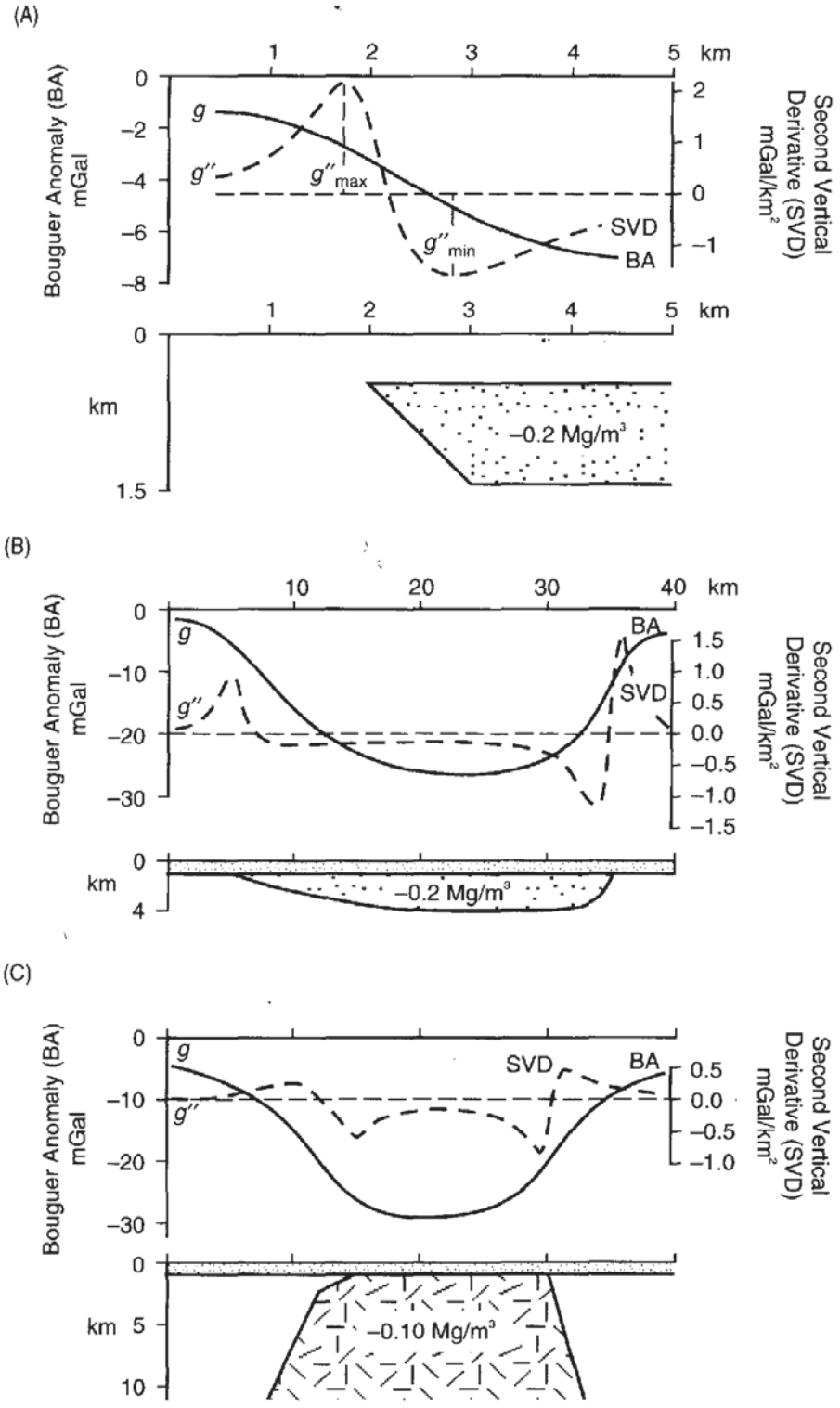

Figure 2.36 Bott criteria to distinguish between the Bouguer gravity profile over (A) a horizontal prism, (B) a sedimentary basin, and (C) a granitic pluton. After Bott (1962), by permission

continued

(2) For a granite pluton:

$$|g''_{max}|/|g''_{min}| \leqslant 1.0.$$

Granite pluton sides slope *outwards*.

The vertical variation of density of sediments with depth in a sedimentary basin can be represented in a number of ways. Moving away from Bott's uniform density model, consideration of the variation in density in terms of exponential and hyperbolic density contrast has been given by Rao *et al.* (1993) and Rao *et al.* (1994), for example.

2.7 APPLICATIONS AND CASE HISTORIES

In this section, a limited number of case histories are described to illustrate the diversity of applications to which the gravity method can be put. Other geophysical methods are discussed as appropriate, where they have been used in conjunction with, or to contrast with, the gravity results. These other methods are explained in their respective chapters.

2.7.1 Exploration of salt domes

2.7.1.1 Mors salt dome, Denmark (waste disposal)

An original interpretation of the Bouguer anomaly (Figure 2.37) over the Mors salt dome in northern Jutland was made in 1974, five years before any seismic results were known (Sharma, 1986). The investigation was connected to a feasibility study for the safe disposal of radioactive waste in the salt dome, but the methodology is identical had the study been for hydrocarbons.

The salt dome was approximated by a sphere. The values of $\Delta g_{max} \approx 16$ mGal and the half-width ≈ 3.7 km were obtained from profiles across the feature (Figure 2.38A) used to determine the depth to the centre of mass ($z = 4.8$ km). In order to calculate the depth to the top of the sphere, an estimate of the density contrast of the salt with the surrounding material had to be made. For a density contrast ($\delta\rho$) of -0.25 Mg/m^3, this gave the radius of the sphere as 3.8 km and thus depth to the top of the sphere is about 1 km (4.8 km minus 3.8 km); with $\delta\rho = -0.2$ Mg/m^3, the radius is 4.1 km and depth to the top is 0.7 km (4.8 km -4.1 km). This was later found to be in good agreement with the seismic results (Figure 2.38B). If the salt dome approximated to a vertical cylinder of length 5300 m, depth to top 700 m, and radius 4400 m, and density contrast -0.2 Mg/m^3, the expected value of Δg_{max} is around 19 mGal, compared with an observed value of 16–18 mGal; but this is still close enough to be a reasonable approximation to the actual shape.